

Electron-Doping Effect on the Magnetic-Field-Sensitive Dielectric Anomaly in $\text{CaMn}_{1-x}\text{Sb}_x\text{O}_3$

Haruka Taniguchi¹, Hidenori Takahashi¹, Akihiro Terui¹, Satoru Kobayashi¹,
Michiaki Matsukawa¹, and Ramanathan Suryanarayanan²

¹Department of Physical Science and Materials Engineering, Iwate University, Morioka 020-8551, Japan

²ICMMO, Université Paris-Sud, 91405 Orsay, France

We measured the temperature dependence of the dielectric constant of the electron-doped manganite $\text{CaMn}_{1-x}\text{Sb}_x\text{O}_3$ ($x = 0.1, 0.12, 0.13, 0.15,$ and 0.2). The real part exhibits a broad peak and the imaginary part exhibits a shoulder structure at a lower temperature in all the samples, suggesting a gradual growth of clusters which has a dipole ordering. We newly revealed that the temperatures of these dielectric anomalies are enhanced by more than 90 K by the Sb substitution from $x = 0.1$ to $x = 0.2$. The result indicates that the carrier concentration should be a decisive parameter for the dipole ordering in $\text{CaMn}_{1-x}\text{Sb}_x\text{O}_3$. Moreover, a magnetocapacitive effect is observed in all the samples.

Index Terms—Dielectric constant, relaxor ferroelectrics.

I. INTRODUCTION

MANGANITES exhibit a wide variety of electronic phases because of electron interactions [for example, the competition between ferromagnetic double exchange interaction and antiferromagnetic (AFM) superexchange interaction]. Carrier doping is one of the powerful tools to control the electronic states. For example, an electron-doped system $\text{CaMn}_{1-x}\text{Mo}_x\text{O}_3$ changes the ground state from a G-type AFM ordering to a charge/orbital-ordered C-type AFM ordering [1], [2]. In another electron-doped system $\text{Ca}_{1-x}\text{La}_x\text{MnO}_3$, dielectric properties are reported [3], [4]. Moreover, in hole-doped systems such as $\text{Pr}_{1-x}\text{Ca}_x\text{MnO}_3$ and $\text{Y}_{1-x}\text{Ca}_x\text{MnO}_3$ [5]–[9], the temperature dependence of the real part of the dielectric constant exhibits a peak which is sensitive to a magnetic field around the charge-ordering (CO) temperature.

Aiming to discover new phenomena in manganites, our group has investigated an electron-doped system $\text{CaMn}_{1-x}\text{Sb}_x\text{O}_3$ for $x \leq 0.1$ [10]–[13]. The result of X-ray photoelectron spectroscopy indicates that the valence of Sb is $5+$ [12]. Thus, the substitution of Sb^{5+} ion for Mn^{4+} site causes one-electron doping with the chemical formula $\text{Ca}^{2+}\text{Mn}_{1-2x}^{4+}\text{Mn}_x^{3+}\text{Sb}_x^{5+}\text{O}_3^{2-}$ accompanied by a monotonic increase of unit-cell volume as a function of x . The magnetization and ac susceptibility measurements suggest a canted AFM ordering below about 100 K [10]–[13], although the long-range order might be suppressed by the substitutional disorder. Interestingly, a magnetization reversal is observed after a field cooling for $0.02 \leq x \leq 0.08$ [10], [11]. We consider that the local lattice distortion of MnO_6 octahedra induced by the Sb substitution changes the orbital state of the e_g electron of Mn^{3+} and reverses the local easy axis of the magnetization.

Manuscript received June 15, 2018; revised August 6, 2018; accepted August 30, 2018. Corresponding author: H. Taniguchi (e-mail: tanig@iwate-u.ac.jp).

Color versions of one or more of the figures in this paper are available online at <http://ieeexplore.ieee.org>.

Digital Object Identifier 10.1109/TMAG.2018.2868511

For $x = 0.05$, the physical and chemical pressure effect is also studied [12], [13].

Just recently, we investigated the dielectric properties of $\text{CaMn}_{0.85}\text{Sb}_{0.15}\text{O}_3$ [14], [15], because manganites provide interesting dielectric materials, such as multiferroics and relaxors. A broad and large peak is found in the temperature dependence of the dielectric constant. Surprisingly, the peak is sensitive to a magnetic field. One candidate for this magnetic-field effect is the magnetoelectric effect in multiferroics. Many multiferroics have been really discovered in manganites, such as YMnO_3 , TbMnO_3 , and MnWO_4 [16]–[22]. Inhomogeneous systems, such as a relaxor $\text{Pb}(\text{Fe}_{1/2}\text{Nb}_{1/2})\text{O}_3$, can be a multiferroic material as well [23]. In relaxors, the polar nanoregions embedded in a nonpolar matrix cause a large relative dielectric constant of about 10^4 [24], whereas the homogeneous multiferroics, such as TbMnO_3 , usually exhibit ϵ' of about 10.

In this paper, in order to reveal the carrier-concentration effect on the dielectric properties of the $\text{CaMn}_{1-x}\text{Sb}_x\text{O}_3$ system, we have newly synthesized polycrystalline $\text{CaMn}_{1-x}\text{Sb}_x\text{O}_3$ ($x = 0.1, 0.12, 0.13, 0.15,$ and 0.2) and measured the dielectric constant. In all the samples, we observed a relaxor-like broad peak in the temperature dependence of the real part, which is followed by an anomaly of the imaginary part. Notably, the characteristic temperatures of the dielectric anomalies are remarkably enhanced by more than 90 K with increasing the carrier concentration. This drastic change of the anomaly temperatures indicates that the carrier concentration is a crucial parameter for the dielectric properties in the $\text{CaMn}_{1-x}\text{Sb}_x\text{O}_3$ system. Moreover, all the samples exhibit a magnetocapacitive effect: the peak of the real part is suppressed by a magnetic field of 1 T.

II. EXPERIMENT

The polycrystalline samples of $\text{CaMn}_{1-x}\text{Sb}_x\text{O}_3$ ($x = 0.1, 0.12, 0.13, 0.15,$ and 0.2) were prepared by a solid-state reaction method [14]. The stoichiometric mixtures of CaCO_3 ,

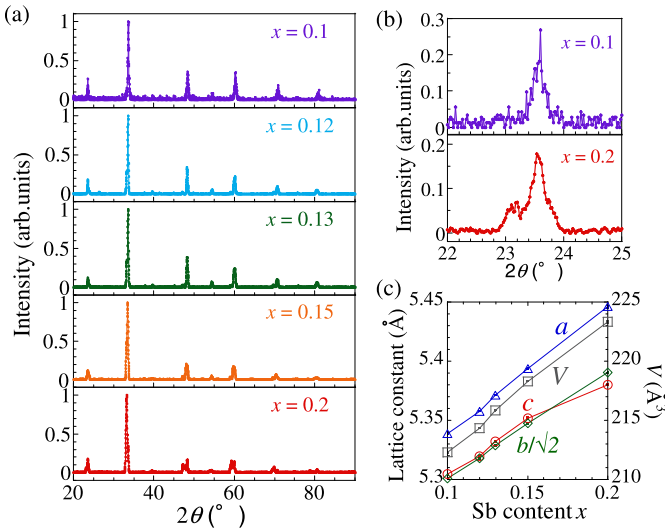


Fig. 1. (a) X-ray diffraction spectrum of $\text{CaMn}_{1-x}\text{Sb}_x\text{O}_3$ ($x = 0.1, 0.12, 0.13, 0.15, \text{ and } 0.2$). (b) Enlarged view around the (101) peak for $x = 0.1$ and 0.2 . (c) Lattice constants and unit cell volume of $\text{CaMn}_{1-x}\text{Sb}_x\text{O}_3$ with error bars.

number of larger Sb^{5+} and Mn^{3+} ions whose ionic radius is 0.60 and 0.645 Å, respectively [26].

In Fig. 2(a) and (b), we compare the temperature dependence of the dielectric constant among $\text{CaMn}_{1-x}\text{Sb}_x\text{O}_3$ ($x = 0.1, 0.12, 0.13, 0.15, \text{ and } 0.2$), which is measured under a magnetic field of 0 T and an ac voltage of 1 V/mm and 100 kHz. We have revealed that all the samples exhibit a broad peak in the real part ϵ' and a shoulder structure in the imaginary part ϵ'' . Interestingly, both of these dielectric anomalies are shifted to a higher temperature by increasing the Sb content. The values of ϵ' and ϵ'' in Fig. 2 are normalized to be 1 at the peak temperature of ϵ' . The raw value of the real part of the relative dielectric constant ϵ_r is 10^3 – 10^4 at the peak, whereas the raw value of the imaginary part of ϵ_r drastically changes on cooling from 10^4 – 10^5 to 1 – 10^2 . Except for the shoulder structure, the temperature dependence of ϵ'' seems to be roughly described by a power law. The electrical resistivity ρ of $\text{CaMn}_{1-x}\text{Sb}_x\text{O}_3$ is smaller than that of the typical insulators by several orders of magnitude, although its temperature dependence is described by the band-gap model $\rho \propto \rho_0 \exp(\Delta/k_B T)$. Therefore, the dielectric loss of $\text{CaMn}_{1-x}\text{Sb}_x\text{O}_3$ is expected to exhibit an extremely large value at higher temperatures and to be suppressed remarkably on cooling; the large values of ϵ'' at higher temperatures and its quasi-power-law temperature dependence would be originated from the conduction current. Comparably large ϵ'' is really observed in a low resistivity system $\text{Pr}_{1-x}\text{Ca}_x\text{MnO}_3$ [27]. Therefore, we consider that the shoulder structure in $\epsilon''(T)$ is a peak appeared on a quasi-power-law background.

We estimate the characteristic temperatures of the dielectric anomalies as follows and plot them in Fig. 2(c). The temperature at which ϵ' exhibits a maximum value is defined as the peak temperature of the real part T_p . In order to determine the shoulder temperature of ϵ'' , we plot $d\epsilon''/dT(T)$. As shown in the inset of Fig. 2(b), the curve exhibits one minimum and one maximum. Since the minimum of $d\epsilon''/dT(T)$ is expected to correspond to the middle of the shoulder in $\epsilon''(T)$, we define the temperature of this minimum as the shoulder temperature of the imaginary part T_s .

In this paper, we have newly clarified that both T_p and T_s are almost linearly enhanced by more than 90 K from $x = 0.1$ to 0.2 . Notably, the drastically enhanced T_s in the Sb substitution in $\text{CaMn}_{1-x}\text{Sb}_x\text{O}_3$ is contrast to the almost unchanged T_s in the Sr substitution in $\text{Ca}_{1-y}\text{Sr}_y\text{Mn}_{0.85}\text{Sb}_{0.15}\text{O}_3$ [15].

We have also investigated the effect of the magnetic field on the dielectric constant of $\text{CaMn}_{1-x}\text{Sb}_x\text{O}_3$ ($x = 0.1, 0.12, 0.13, \text{ and } 0.2$), because we found a magnetocapacitive effect in $\text{CaMn}_{0.85}\text{Sb}_{0.15}\text{O}_3$ [14], [15]. A magnetocapacitive effect was observed in all the samples. A magnetic field of 1 T suppresses the peak value of the real part by 3%–15%. As an example, the result for $\text{CaMn}_{0.88}\text{Sb}_{0.12}\text{O}_3$ is shown in Fig. 3(a). Since we have confirmed that the magnetoresistance effect of $\text{CaMn}_{0.85}\text{Sb}_{0.15}\text{O}_3$ below 4 T is within error margin [15], we consider that these magnetocapacitive effects in $\text{CaMn}_{1-x}\text{Sb}_x\text{O}_3$ are really related to the capacitive carriers.

For $x = 0.1, 0.15, \text{ and } 0.2$, we have studied the frequency dependence of the dielectric constant and found a common tendency. As the result of $x = 0.1$ is shown in Fig. 3(b),

77 SrCO_3 , Mn_3O_4 , and Sb_2O_3 powders were calcined in air at
78 1000 °C for 48 h. The products were ground and pressed
79 into disk-like pellets. The pellets were sintered at 1350 °C
80 for 48 h. We performed the X-ray diffraction measurements at
81 room temperature with an Ultima IV diffractometer (Rigaku)
82 using Cu $K\alpha$ radiation.

83 We measured the temperature dependence of the dielectric
84 constant under the dc magnetic field using the parallel mode
85 of an LCR meter (Agilent, E4980A) [14]. The samples were
86 cut into a parallel plate with a $3.2 \times 6.0 \text{ mm}^2$ area and a
87 0.7 mm thickness, and the Au wires for electric lead were
88 connected by Ag paint (Dupont, 4929N). In order to improve
89 electric conductivity, the sample surfaces were polished to be
90 flat using 9 μm diamond slurry, and the Ag paint was heated
91 at 110 °C for 30 min. We performed measurements with an
92 ac voltage of 1 V/mm and 10, 50, or 100 kHz under 0, 0.01,
93 or 1 T (field cooling), obtained capacitance C and dielectric
94 loss $\tan\delta$, and estimated the real and imaginary parts of the
95 dielectric constant, ϵ' and ϵ'' .

III. RESULTS

97 Fig. 1(a) presents the X-ray diffraction spectrum of
98 $\text{CaMn}_{1-x}\text{Sb}_x\text{O}_3$ ($x = 0.1, 0.12, 0.13, 0.15, \text{ and } 0.2$). The
99 samples of $x \leq 0.15$ present a $Pnma$ orthorhombic structure,
100 whereas the sample of $x = 0.2$ is described by a $P2_1/m$
101 monoclinic structure. As shown in Fig. 1(b), a new peak
102 appears at 23.1° in addition to the peak at 23.5° for $x = 0.2$.
103 The peak at 23.1° is expected to result from the (10–1)
104 reflection, whereas the (101) and (020) reflections are com-
105 bined into one peak at 23.5° . Therefore, the appearance of
106 a peak at 23.1° indicates a structural transition from $Pnma$
107 to $P2_1/m$. This result is consistent with the previous study
108 on $x = 0.1$ and 0.2 [25]. The obtained lattice parameters and
109 unit cell volume are plotted in Fig. 1(c). The values of a , b ,
110 and c exhibit an almost linear increase with increasing the Sb
111 content x . This substitution effect on the lattice is reasonable:
112 the Sb substitution decreases the number of smaller Mn^{4+} ions
113 whose ionic radius is 0.530 Å, whereas it increases the

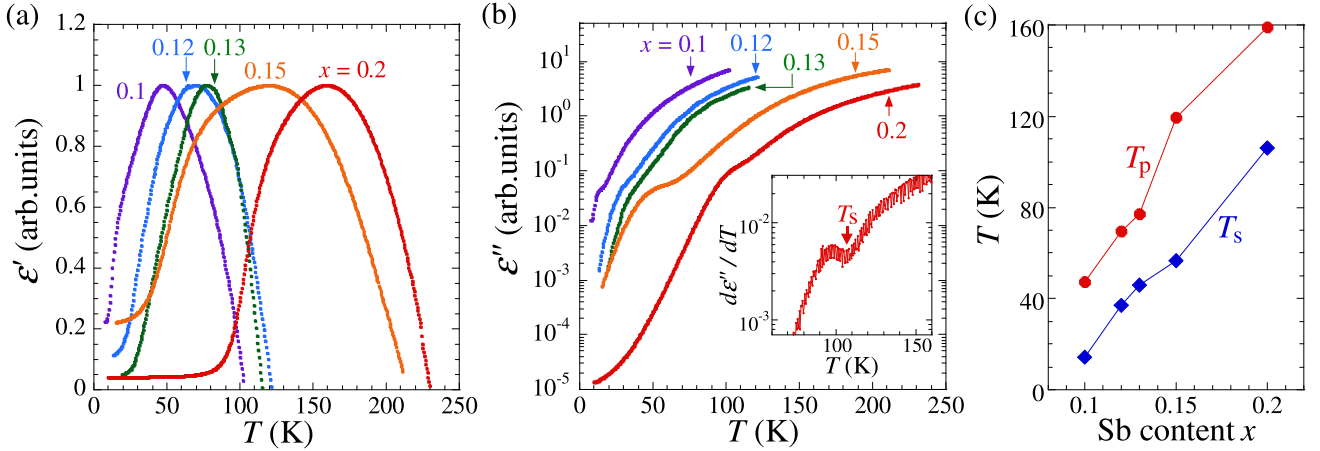


Fig. 2. Temperature dependence of the dielectric constant of $\text{CaMn}_{1-x}\text{Sb}_x\text{O}_3$ ($x = 0.1, 0.12, 0.13, 0.15,$ and 0.2) (an ac voltage of 1 V/mm and 100 kHz, 0 T). (a) Real part ϵ' . (b) Imaginary part ϵ'' . The inset of (b) is the temperature dependence of $d\epsilon''/dT$ for $x = 0.2$. The arrow indicates the minimum of which temperature is defined as the shoulder temperature T_s . (c) Sb content dependence of the characteristic temperatures of the dielectric anomalies in $\text{CaMn}_{1-x}\text{Sb}_x\text{O}_3$, which are determined from the measurements of (a) and (b). T_p (circle) is the peak temperature of the real part, whereas T_s (diamond) is the shoulder temperature of the imaginary part.

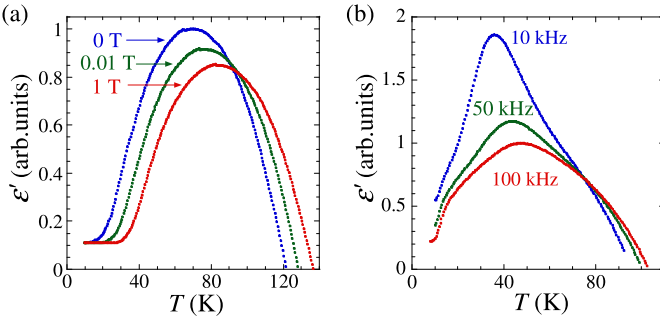


Fig. 3. (a) Magnetocapacitive effect in the real part of the dielectric constant ϵ' of $\text{CaMn}_{0.88}\text{Sb}_{0.12}\text{O}_3$ (an ac voltage of 1 V/mm and 100 kHz). (b) Frequency dependence of ϵ' of $\text{CaMn}_{0.9}\text{Sb}_{0.1}\text{O}_3$ (0 T, 1 V/mm).

the peak of $\epsilon'(T)$ is suppressed and shifted to a higher temperature with an increasing frequency.

IV. DISCUSSION

As discussed for $\text{CaMn}_{0.85}\text{Sb}_{0.15}\text{O}_3$ [14], [15], the peak structure of $\epsilon'(T)$ in $\text{CaMn}_{1-x}\text{Sb}_x\text{O}_3$ ($0.1 \leq x \leq 0.2$) suggests that it becomes difficult for the dipole moments to follow the plus-minus switching of an applied ac voltage below T_p . This behavior can be interpreted as the result of a spontaneous dipole ordering. The large value and the broad peak of ϵ' as well as its frequency dependence suggest that $\text{CaMn}_{1-x}\text{Sb}_x\text{O}_3$ is a relaxor in which the polar nanoregions exist in a non-polar matrix [24]. The inevitable disorder induced by substitution is consistent with the relaxor scenario. Since the shoulder structure of $\epsilon''(T)$ is understood as a peak appeared on a quasi-power-law background, the shoulder is expected to indicate a dielectric energy dissipation. These results in $\text{CaMn}_{1-x}\text{Sb}_x\text{O}_3$ ($0.1 \leq x \leq 0.2$) suggest that local dipole-ordering clusters which start to form at T_p expand remarkably around T_s for an energy dissipation to be detectable in ϵ'' . Since some relaxors exhibit ferroelectricity much below the peak temperature of $\epsilon'(T)$, it is expected to be reasonable for dipole-ordering clusters to grow gradually on cooling.

The suppression of the peak height of ϵ' by a magnetic field suggests that the response of dipole moments to an applied

ac voltage is interfered by the magnetic field. In other words, a spontaneous dipole ordering along a certain direction is stabilized by a magnetic field.

In order to discuss the origin of the dielectric anomalies and the magnetocapacitive effect in $\text{CaMn}_{1-x}\text{Sb}_x\text{O}_3$, the $x - T$ phase diagram would be important. Focusing on the dielectric properties, we have newly revealed that T_p and T_s are almost linearly enhanced from $x = 0.1$ to 0.2 . On other properties such as the magnetic phase, we can speculate based on the phase diagram of the similar carrier-doped manganites. Comparing the one-electron-doped system $\text{CaMn}_{1-x}\text{Sb}_x\text{O}_3$ with a two-electron-doped system $\text{AeMn}_{1-z}\text{Mo}_z\text{O}_3$ (Ae : Alkaline earth metal), from the viewpoint of the average valence α of Mn ions, $\text{CaMn}_{0.85}\text{Sb}_{0.15}\text{O}_3$ with $\alpha = +3.82$ and $\text{CaMn}_{0.8}\text{Sb}_{0.2}\text{O}_3$ with $\alpha = +3.75$ correspond to $\text{AeMn}_{0.917}\text{Mo}_{0.083}\text{O}_3$ and $\text{AeMn}_{0.889}\text{Mo}_{0.111}\text{O}_3$, respectively. Considering that the structural phase transition from $Pnma$ to $P2_1/m$ at the room temperature occurs between $\text{CaMn}_{0.85}\text{Sb}_{0.15}\text{O}_3$ and $\text{CaMn}_{0.8}\text{Sb}_{0.2}\text{O}_3$, the phase diagram of $\text{CaMn}_{1-x}\text{Sb}_x\text{O}_3$ is expected to be similar to that of $\text{Ca}_{0.75}\text{Sr}_{0.25}\text{Mn}_{1-z}\text{Mo}_z\text{O}_3$ in which the same structural transition occurs between $z = 0.083$ and 0.111 [2]. In the phase diagram of $\text{Ca}_{0.75}\text{Sr}_{0.25}\text{Mn}_{1-z}\text{Mo}_z\text{O}_3$, the ground state for $0.052 \leq z \leq 0.111$, which corresponds to $0.1 \leq x \leq 0.2$ in $\text{CaMn}_{1-x}\text{Sb}_x\text{O}_3$, is the C-type AFM phase with charge/orbital ordering, whose ordering temperature is linearly enhanced by more than 130 K in this range. In $\text{CaMn}_{0.85}\text{Sb}_{0.15}\text{O}_3$, we really observed a magnetic anomaly that suggests a CO near T_p [14], [15].

Therefore, the dielectric peak in $\text{CaMn}_{1-x}\text{Sb}_x\text{O}_3$, which indicates the formation of a dipole ordering, is expected to have a positive correlation with a charge/orbital ordering. As for the magnetocapacitive effect, since charge/orbital orderings in CaMnO_3 series stabilize a certain magnetic ordering [28], we consider that the dipole ordering related to a charge/orbital ordering is affected by a magnetic field through a magnetic ordering. This magnetic-field-sensitive dielectric peak, which seems to be related to a charge/orbital ordering, is similar to that in the hole-doped system $\text{Pr}_{1-x}\text{Ca}_x\text{MnO}_3$ and

237 $Y_{1-x}Ca_xMnO_3$ [5]–[9], but it is the first example among
238 electron-doped $CaMnO_3$ systems.

239 Concerning the dielectric anomaly in the imaginary
240 part which indicates the active development of electri-
241 cally polarized regions, T_s is notably sensitive to the one-
242 electron-doping Sb substitution in $CaMn_{1-x}Sb_xO_3$, whereas
243 it is not affected by the isovalent Sr substitution in
244 $Ca_{1-y}Sr_yMn_{0.85}Sb_{0.15}O_3$ [15]. From these contrast results,
245 we emphasize that the carrier concentration is a crucial
246 parameter for the expansion of polar nanoregions in the
247 $Ca_{1-y}Sr_yMn_{1-x}Sb_xO_3$ system.

248 As a next issue, it would be important to clarify whether
249 macroscopic electric polarization exists at low temperatures.
250 In order to check our scenario on the mechanism of the
251 dipole anomalies and the magnetocapacitive effect in the
252 $Ca_{1-y}Sr_yMn_{1-x}Sb_xO_3$ system, the magnetic ground state and
253 the possibility of a charge/orbital ordering should be studied.

254 V. CONCLUSION

255 We measured the dielectric constant of the electron-doped
256 manganite $CaMn_{1-x}Sb_xO_3$ ($x = 0.1, 0.12, 0.13, 0.15,$
257 $\text{and } 0.2$). The temperature dependence of the real part exhibits
258 a broad and large peak of which value is suppressed and
259 of which temperature is enhanced by increasing frequency,
260 whereas the imaginary part shows a shoulder anomaly on a
261 quasi-power-law temperature dependence. These results sug-
262 gest that $CaMn_{1-x}Sb_xO_3$ is a relaxor: clusters with a short-
263 range dipole ordering appear at the peak temperature and grow
264 gradually, especially actively at the shoulder temperature.

265 Importantly, we have revealed that the shoulder temperature
266 is remarkably enhanced with the increasing Sb content x .
267 This result indicates that the growth of the clusters is strongly
268 affected by the carrier concentration. Moreover, the dielectric
269 peak is sensitive to a magnetic field in all the samples. By anal-
270 ogy with other $CaMnO_3$ systems, a charge/orbital ordering and
271 an accompanying magnetic ordering might play an important
272 role for the dielectric ordering in $CaMn_{1-x}Sb_xO_3$.

273 ACKNOWLEDGMENT

274 The authors would like to thank Y. Ishii, H. Yamamoto,
275 S. Sekigawa, and H. Kimura for their fruitful discussions. This
276 work was supported in part by Iwate University and in part
277 by JSPS KAKENHI Grant Number JP17K14101.

278 REFERENCES

279 [1] A. Maignan, C. Martin, C. Autret, M. Hervieu, B. Raveau, and
280 J. Hejtmanek, "Structural–magnetic phase diagram of Mo-substituted
281 $CaMnO_3$: Consequences for thermoelectric power properties," *J. Mater.*
282 *Chem.*, vol. 12, no. 6, pp. 1806–1811, 2002.
283 [2] T. Okuda and Y. Fujii, "Cosubstitution effect on the magnetic, transport,
284 and thermoelectric properties of the electron-doped perovskite manganite
285 $CaMnO_3$," *J. Appl. Phys.*, vol. 108, no. 10, p. 103702, 2010.
286 [3] J. L. Cohn, M. Peterca, and J. J. Neumeier, "Low-temperature permittivity
287 of insulating perovskite manganites," *Phys. Rev. B, Condens. Matter*,
288 vol. 70, no. 21, p. 214433, 2004.
289 [4] J. L. Cohn, M. Peterca, and J. J. Neumeier, "Giant dielectric per-
290 mittivity of electron-doped manganite thin films, $Ca_{1-x}La_xMnO_3$
291 ($0 \leq x \leq 0.03$)," *J. Appl. Phys.*, vol. 97, no. 3, p. 034102, 2005.
292 [5] C. Jardón *et al.*, "Experimental study of charge ordering transi-
293 tion in $Pr_{0.67}Ca_{0.33}MnO_3$," *J. Magn. Magn. Mater.*, vols. 196–197,
294 pp. 475–476, May 1999.

295 [6] S. Mercene, A. Wahl, A. Pautrat, M. Pollet, and C. Simon, "Anomaly
296 in the dielectric response at the charge-orbital-ordering transition of
297 $Pr_{0.67}Ca_{0.33}MnO_3$," *Phys. Rev. B, Condens. Matter*, vol. 69, p. 174433,
298 May 2004.
299 [7] R. S. Freitas, J. F. Mitchell, and P. Schiffer, "Magnetodielectric conse-
300 quences of phase separation in the colossal magnetoresistance manganite
301 $Pr_{0.7}Ca_{0.3}MnO_3$," *Phys. Rev. B, Condens. Matter*, vol. 72, no. 14,
302 p. 144429, 2005.
303 [8] C. R. Serrao, A. Sundaresan, and C. N. R. Rao, "Multiferroic nature
304 of charge-ordered rare earth manganites," *J. Phys., Condens. Matter*,
305 vol. 19, p. 496217, 2007.
306 [9] J. R. Sahu, C. R. Serrao, A. Ghosh, A. Sundaresan, and C. N. R. Rao,
307 "Charge-order-driven multiferroic properties of $Y_{1-x}Ca_xMnO_3$," *Solid*
308 *State Commun.*, vol. 149, pp. 49–51, Jan. 2009.
309 [10] Y. Murano, M. Matsukawa, S. Kobayashi, S. Nimori, and
310 R. Suryanarayanan, "Transport and magnetic properties of electron-
311 doped manganites $CaMn_{1-x}Sb_xO_3$," *J. Phys., Conf. Ser.*, vol. 200,
312 no. 1, p. 012114, 2010.
313 [11] Y. Murano *et al.*, "Effect of pressure on the magnetic, transport,
314 and thermal-transport properties of the electron-doped manganite
315 $CaMn_{1-x}Sb_xO_3$," *Phys. Rev. B, Condens. Matter*, vol. 83, p. 054437,
316 Feb. 2011.
317 [12] T. Fujiwara, M. Matsukawa, S. Ohuchi, S. Kobayashi, S. Nimori, and
318 R. Suryanarayanan, "Magnetization reversal and chemical pressure effect
319 in the electron-doped manganite $CaMn_{0.95}Sb_{0.05}O_3$," *J. Kor. Phys. Soc.*,
320 vol. 62, p. 1925, 2013.
321 [13] T. Fujiwara *et al.*, "Magnetic and thermodynamic properties of the
322 lightly electron-doped manganite compound $(Ca,Sr)Mn_{0.95}Sb_{0.05}O_3$,"
323 *J. Magn. Magn. Mater.*, vol. 378, pp. 451–456, Mar. 2015.
324 [14] H. Taniguchi, H. Takahashi, A. Terui, S. Kobayashi, M. Matsukawa,
325 and R. Suryanarayanan, "Dielectric anomaly and magnetoelectric effect
326 accompanying a charge ordering in the electron-doped manganite
327 $Ca_{1-x}Sr_xMn_{0.85}Sb_{0.15}O_3$," *J. Phys., Conf. Ser.*, vol. 969, no. 1,
328 p. 012094, 2018.
329 [15] H. Taniguchi, H. Takahashi, A. Terui, S. Kobayashi, M. Matsukawa,
330 and R. Suryanarayanan, "Relaxor-like dielectric anomaly and magneto-
331 capacitive effect in electron-doped $Ca_{1-x}Sr_xMn_{0.85}Sb_{0.15}O_3$," submit-
332 ted for publication.
333 [16] M. Fiebig, T. Lottermoser, D. Fröhlich, A. V. Goltsev, and
334 R. V. Pisarev, "Observation of coupled magnetic and electric domains,"
335 *Nature*, vol. 419, pp. 818–820, Oct. 2002.
336 [17] B. Lorenz, Y.-Q. Wang, and C.-W. Chu, "Ferroelectricity in perovskite
337 $HoMnO_3$ and $YMnO_3$," *Phys. Rev. B, Condens. Matter*, vol. 76, no. 10,
338 p. 104405, 2007.
339 [18] T. Kimura, T. Goto, H. Shintani, K. Ishizaka, T. Arima, and Y. Tokura,
340 "Magnetic control of ferroelectric polarization," *Nature*, vol. 426,
341 pp. 55–58, Nov. 2003.
342 [19] M. Kenzelmann *et al.*, "Magnetic inversion symmetry breaking and
343 ferroelectricity in $TbMnO_3$," *Phys. Rev. Lett.*, vol. 95, no. 8, p. 087206,
344 2005.
345 [20] A. H. Arkenbout, T. T. M. Palstra, T. Siegrist, and T. Kimura, "Ferro-
346 electricity in the cycloidal spiral magnetic phase of $MnWO_4$," *Phys.*
347 *Rev. B, Condens. Matter*, vol. 74, no. 18, p. 184431, 2006.
348 [21] O. Heyer *et al.*, "A new multiferroic material: $MnWO_4$," *J. Phys.,*
349 *Condens. Matter*, vol. 18, no. 39, p. L471, 2006.
350 [22] K. Taniguchi, N. Abe, T. Takenobu, Y. Iwasa, and T. Arima, "Ferro-
351 electric polarization flop in a frustrated magnet $MnWO_4$ induced by a
352 magnetic field," *Phys. Rev. Lett.*, vol. 97, p. 097203, Aug. 2006.
353 [23] W. Kleemann, V. V. Shvartsman, P. Borisov, and A. Kania, "Coexistence
354 of antiferromagnetic and spin cluster glass order in the magnetoelec-
355 tric relaxor multiferroic $PbFe_{0.5}Nb_{0.5}O_3$," *Phys. Rev. Lett.*, vol. 105,
356 p. 257202, Dec. 2010.
357 [24] A. A. Bokov and Z.-G. Ye, "Recent progress in relaxor ferroelectrics
358 with perovskite structure," *J. Mater. Sci.*, vol. 41, no. 1, pp. 31–52, 2006.
359 [25] V. Poltavets, K. Vidyasagar, and M. Jansen, "Crystal structures and
360 magnetic properties of $CaSb_xMn_{1-x}O_3$ perovskites," *Solid State Chem.*,
361 vol. 177, pp. 1285–1291, Apr./May 2004.
362 [26] R. D. Shannon, "Revised effective ionic radii and systematic studies
363 of interatomic distances in halides and chalcogenides," *Acta Cryst.*,
364 vol. 32, pp. 751–767, Sep. 1976.
365 [27] V. K. Shukla, S. Mukhopadhyay, K. Das, A. Sarma, and I. Das, "Direct
366 experimental evidence of multiferroicity in a nanocrystalline Zener
367 polaron ordered manganite," *Phys. Rev. B, Condens. Matter*, vol. 90,
368 no. 24, p. 245126, 2014.
369 [28] E. N. Caspi *et al.*, "Structural and magnetic phase diagram of the
370 two-electron-doped $(Ca_{1-x}Ce_x)MnO_3$ system: Effects of competition
371 among charge, orbital, and spin ordering," *Phys. Rev. B, Condens.*
372 *Matter*, vol. 69, no. 10, p. 104402, 2004.

Electron-Doping Effect on the Magnetic-Field-Sensitive Dielectric Anomaly in $\text{CaMn}_{1-x}\text{Sb}_x\text{O}_3$

Haruka Taniguchi¹, Hidenori Takahashi¹, Akihiro Terui¹, Satoru Kobayashi¹,
Michiaki Matsukawa¹, and Ramanathan Suryanarayanan²

¹Department of Physical Science and Materials Engineering, Iwate University, Morioka 020-8551, Japan

²ICMMO, Université Paris-Sud, 91405 Orsay, France

We measured the temperature dependence of the dielectric constant of the electron-doped manganite $\text{CaMn}_{1-x}\text{Sb}_x\text{O}_3$ ($x = 0.1, 0.12, 0.13, 0.15,$ and 0.2). The real part exhibits a broad peak and the imaginary part exhibits a shoulder structure at a lower temperature in all the samples, suggesting a gradual growth of clusters which has a dipole ordering. We newly revealed that the temperatures of these dielectric anomalies are enhanced by more than 90 K by the Sb substitution from $x = 0.1$ to $x = 0.2$. The result indicates that the carrier concentration should be a decisive parameter for the dipole ordering in $\text{CaMn}_{1-x}\text{Sb}_x\text{O}_3$. Moreover, a magnetocapacitive effect is observed in all the samples.

Index Terms—Dielectric constant, relaxor ferroelectrics.

I. INTRODUCTION

MANGANITES exhibit a wide variety of electronic phases because of electron interactions [for example, the competition between ferromagnetic double exchange interaction and antiferromagnetic (AFM) superexchange interaction]. Carrier doping is one of the powerful tools to control the electronic states. For example, an electron-doped system $\text{CaMn}_{1-x}\text{Mo}_x\text{O}_3$ changes the ground state from a G-type AFM ordering to a charge/orbital-ordered C-type AFM ordering [1], [2]. In another electron-doped system $\text{Ca}_{1-x}\text{La}_x\text{MnO}_3$, dielectric properties are reported [3], [4]. Moreover, in hole-doped systems such as $\text{Pr}_{1-x}\text{Ca}_x\text{MnO}_3$ and $\text{Y}_{1-x}\text{Ca}_x\text{MnO}_3$ [5]–[9], the temperature dependence of the real part of the dielectric constant exhibits a peak which is sensitive to a magnetic field around the charge-ordering (CO) temperature.

Aiming to discover new phenomena in manganites, our group has investigated an electron-doped system $\text{CaMn}_{1-x}\text{Sb}_x\text{O}_3$ for $x \leq 0.1$ [10]–[13]. The result of X-ray photoelectron spectroscopy indicates that the valence of Sb is $5+$ [12]. Thus, the substitution of Sb^{5+} ion for Mn^{4+} site causes one-electron doping with the chemical formula $\text{Ca}^{2+}\text{Mn}_{1-2x}^{4+}\text{Mn}_x^{3+}\text{Sb}_x^{5+}\text{O}_3^{2-}$ accompanied by a monotonic increase of unit-cell volume as a function of x . The magnetization and ac susceptibility measurements suggest a canted AFM ordering below about 100 K [10]–[13], although the long-range order might be suppressed by the substitutional disorder. Interestingly, a magnetization reversal is observed after a field cooling for $0.02 \leq x \leq 0.08$ [10], [11]. We consider that the local lattice distortion of MnO_6 octahedra induced by the Sb substitution changes the orbital state of the e_g electron of Mn^{3+} and reverses the local easy axis of the magnetization.

Manuscript received June 15, 2018; revised August 6, 2018; accepted August 30, 2018. Corresponding author: H. Taniguchi (e-mail: tanig@iwate-u.ac.jp).

Color versions of one or more of the figures in this paper are available online at <http://ieeexplore.ieee.org>.

Digital Object Identifier 10.1109/TMAG.2018.2868511

For $x = 0.05$, the physical and chemical pressure effect is also studied [12], [13].

Just recently, we investigated the dielectric properties of $\text{CaMn}_{0.85}\text{Sb}_{0.15}\text{O}_3$ [14], [15], because manganites provide interesting dielectric materials, such as multiferroics and relaxors. A broad and large peak is found in the temperature dependence of the dielectric constant. Surprisingly, the peak is sensitive to a magnetic field. One candidate for this magnetic-field effect is the magnetoelectric effect in multiferroics. Many multiferroics have been really discovered in manganites, such as YMnO_3 , TbMnO_3 , and MnWO_4 [16]–[22]. Inhomogeneous systems, such as a relaxor $\text{Pb}(\text{Fe}_{1/2}\text{Nb}_{1/2})\text{O}_3$, can be a multiferroic material as well [23]. In relaxors, the polar nanoregions embedded in a nonpolar matrix cause a large relative dielectric constant of about 10^4 [24], whereas the homogeneous multiferroics, such as TbMnO_3 , usually exhibit ϵ' of about 10.

In this paper, in order to reveal the carrier-concentration effect on the dielectric properties of the $\text{CaMn}_{1-x}\text{Sb}_x\text{O}_3$ system, we have newly synthesized polycrystalline $\text{CaMn}_{1-x}\text{Sb}_x\text{O}_3$ ($x = 0.1, 0.12, 0.13, 0.15,$ and 0.2) and measured the dielectric constant. In all the samples, we observed a relaxor-like broad peak in the temperature dependence of the real part, which is followed by an anomaly of the imaginary part. Notably, the characteristic temperatures of the dielectric anomalies are remarkably enhanced by more than 90 K with increasing the carrier concentration. This drastic change of the anomaly temperatures indicates that the carrier concentration is a crucial parameter for the dielectric properties in the $\text{CaMn}_{1-x}\text{Sb}_x\text{O}_3$ system. Moreover, all the samples exhibit a magnetocapacitive effect: the peak of the real part is suppressed by a magnetic field of 1 T.

II. EXPERIMENT

The polycrystalline samples of $\text{CaMn}_{1-x}\text{Sb}_x\text{O}_3$ ($x = 0.1, 0.12, 0.13, 0.15,$ and 0.2) were prepared by a solid-state reaction method [14]. The stoichiometric mixtures of CaCO_3 ,

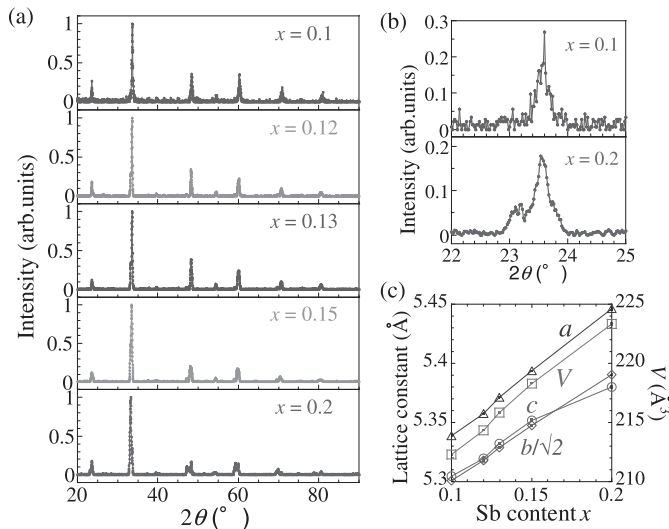


Fig. 1. (a) X-ray diffraction spectrum of $\text{CaMn}_{1-x}\text{Sb}_x\text{O}_3$ ($x = 0.1, 0.12, 0.13, 0.15, \text{ and } 0.2$). (b) Enlarged view around the (101) peak for $x = 0.1$ and 0.2 . (c) Lattice constants and unit cell volume of $\text{CaMn}_{1-x}\text{Sb}_x\text{O}_3$ with error bars.

number of larger Sb^{5+} and Mn^{3+} ions whose ionic radius is 0.60 and 0.645 Å, respectively [26].

In Fig. 2(a) and (b), we compare the temperature dependence of the dielectric constant among $\text{CaMn}_{1-x}\text{Sb}_x\text{O}_3$ ($x = 0.1, 0.12, 0.13, 0.15, \text{ and } 0.2$), which is measured under a magnetic field of 0 T and an ac voltage of 1 V/mm and 100 kHz. We have revealed that all the samples exhibit a broad peak in the real part ϵ' and a shoulder structure in the imaginary part ϵ'' . Interestingly, both of these dielectric anomalies are shifted to a higher temperature by increasing the Sb content. The values of ϵ' and ϵ'' in Fig. 2 are normalized to be 1 at the peak temperature of ϵ' . The raw value of the real part of the relative dielectric constant ϵ_r is 10^3 – 10^4 at the peak, whereas the raw value of the imaginary part of ϵ_r drastically changes on cooling from 10^4 – 10^5 to 1 – 10^2 . Except for the shoulder structure, the temperature dependence of ϵ'' seems to be roughly described by a power law. The electrical resistivity ρ of $\text{CaMn}_{1-x}\text{Sb}_x\text{O}_3$ is smaller than that of the typical insulators by several orders of magnitude, although its temperature dependence is described by the band-gap model $\rho \propto \rho_0 \exp(\Delta/k_B T)$. Therefore, the dielectric loss of $\text{CaMn}_{1-x}\text{Sb}_x\text{O}_3$ is expected to exhibit an extremely large value at higher temperatures and to be suppressed remarkably on cooling; the large values of ϵ'' at higher temperatures and its quasi-power-law temperature dependence would be originated from the conduction current. Comparably large ϵ'' is really observed in a low resistivity system $\text{Pr}_{1-x}\text{Ca}_x\text{MnO}_3$ [27]. Therefore, we consider that the shoulder structure in $\epsilon''(T)$ is a peak appeared on a quasi-power-law background.

We estimate the characteristic temperatures of the dielectric anomalies as follows and plot them in Fig. 2(c). The temperature at which ϵ' exhibits a maximum value is defined as the peak temperature of the real part T_p . In order to determine the shoulder temperature of ϵ'' , we plot $d\epsilon''/dT(T)$. As shown in the inset of Fig. 2(b), the curve exhibits one minimum and one maximum. Since the minimum of $d\epsilon''/dT(T)$ is expected to correspond to the middle of the shoulder in $\epsilon''(T)$, we define the temperature of this minimum as the shoulder temperature of the imaginary part T_s .

In this paper, we have newly clarified that both T_p and T_s are almost linearly enhanced by more than 90 K from $x = 0.1$ to 0.2 . Notably, the drastically enhanced T_s in the Sb substitution in $\text{CaMn}_{1-x}\text{Sb}_x\text{O}_3$ is contrast to the almost unchanged T_s in the Sr substitution in $\text{Ca}_{1-y}\text{Sr}_y\text{Mn}_{0.85}\text{Sb}_{0.15}\text{O}_3$ [15].

We have also investigated the effect of the magnetic field on the dielectric constant of $\text{CaMn}_{1-x}\text{Sb}_x\text{O}_3$ ($x = 0.1, 0.12, 0.13, \text{ and } 0.2$), because we found a magnetocapacitive effect in $\text{CaMn}_{0.85}\text{Sb}_{0.15}\text{O}_3$ [14], [15]. A magnetocapacitive effect was observed in all the samples. A magnetic field of 1 T suppresses the peak value of the real part by 3%–15%. As an example, the result for $\text{CaMn}_{0.88}\text{Sb}_{0.12}\text{O}_3$ is shown in Fig. 3(a). Since we have confirmed that the magnetoresistance effect of $\text{CaMn}_{0.85}\text{Sb}_{0.15}\text{O}_3$ below 4 T is within error margin [15], we consider that these magnetocapacitive effects in $\text{CaMn}_{1-x}\text{Sb}_x\text{O}_3$ are really related to the capacitive carriers.

For $x = 0.1, 0.15, \text{ and } 0.2$, we have studied the frequency dependence of the dielectric constant and found a common tendency. As the result of $x = 0.1$ is shown in Fig. 3(b),

77 SrCO_3 , Mn_3O_4 , and Sb_2O_3 powders were calcined in air at
78 1000 °C for 48 h. The products were ground and pressed
79 into disk-like pellets. The pellets were sintered at 1350 °C
80 for 48 h. We performed the X-ray diffraction measurements at
81 room temperature with an Ultima IV diffractometer (Rigaku)
82 using Cu $K\alpha$ radiation.

83 We measured the temperature dependence of the dielectric
84 constant under the dc magnetic field using the parallel mode
85 of an LCR meter (Agilent, E4980A) [14]. The samples were
86 cut into a parallel plate with a $3.2 \times 6.0 \text{ mm}^2$ area and a
87 0.7 mm thickness, and the Au wires for electric lead were
88 connected by Ag paint (Dupont, 4929N). In order to improve
89 electric conductivity, the sample surfaces were polished to be
90 flat using 9 μm diamond slurry, and the Ag paint was heated
91 at 110 °C for 30 min. We performed measurements with an
92 ac voltage of 1 V/mm and 10, 50, or 100 kHz under 0, 0.01,
93 or 1 T (field cooling), obtained capacitance C and dielectric
94 loss $\tan\delta$, and estimated the real and imaginary parts of the
95 dielectric constant, ϵ' and ϵ'' .

III. RESULTS

97 Fig. 1(a) presents the X-ray diffraction spectrum of
98 $\text{CaMn}_{1-x}\text{Sb}_x\text{O}_3$ ($x = 0.1, 0.12, 0.13, 0.15, \text{ and } 0.2$). The
99 samples of $x \leq 0.15$ present a $Pnma$ orthorhombic structure,
100 whereas the sample of $x = 0.2$ is described by a $P2_1/m$
101 monoclinic structure. As shown in Fig. 1(b), a new peak
102 appears at 23.1° in addition to the peak at 23.5° for $x = 0.2$.
103 The peak at 23.1° is expected to result from the (10–1)
104 reflection, whereas the (101) and (020) reflections are com-
105 bined into one peak at 23.5° . Therefore, the appearance of
106 a peak at 23.1° indicates a structural transition from $Pnma$
107 to $P2_1/m$. This result is consistent with the previous study
108 on $x = 0.1$ and 0.2 [25]. The obtained lattice parameters and
109 unit cell volume are plotted in Fig. 1(c). The values of a , b ,
110 and c exhibit an almost linear increase with increasing the Sb
111 content x . This substitution effect on the lattice is reasonable:
112 the Sb substitution decreases the number of smaller Mn^{4+} ions
113 whose ionic radius is 0.530 Å, whereas it increases the

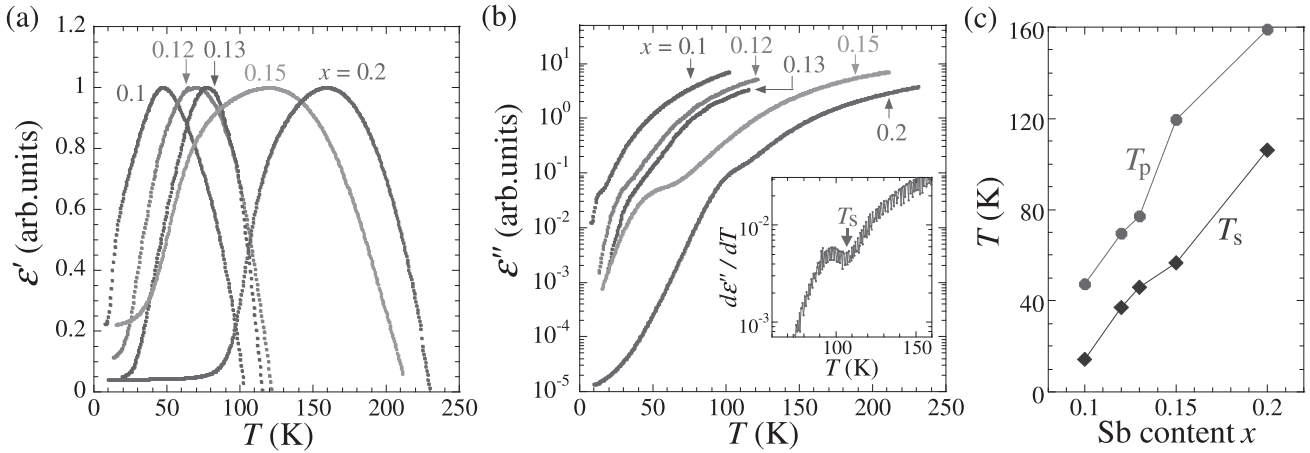


Fig. 2. Temperature dependence of the dielectric constant of $\text{CaMn}_{1-x}\text{Sb}_x\text{O}_3$ ($x = 0.1, 0.12, 0.13, 0.15,$ and 0.2) (an ac voltage of 1 V/mm and 100 kHz, 0 T). (a) Real part ϵ' . (b) Imaginary part ϵ'' . The inset of (b) is the temperature dependence of $d\epsilon''/dT$ for $x = 0.2$. The arrow indicates the minimum of which temperature is defined as the shoulder temperature T_s . (c) Sb content dependence of the characteristic temperatures of the dielectric anomalies in $\text{CaMn}_{1-x}\text{Sb}_x\text{O}_3$, which are determined from the measurements of (a) and (b). T_p (circle) is the peak temperature of the real part, whereas T_s (diamond) is the shoulder temperature of the imaginary part.

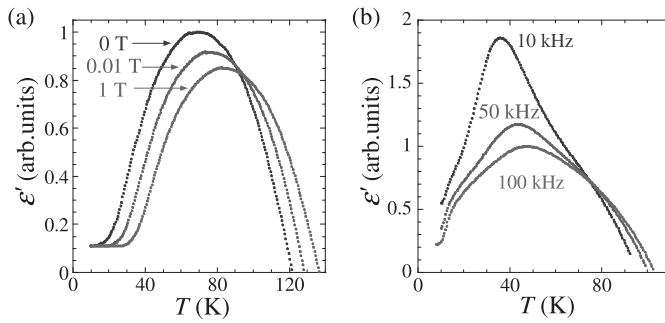


Fig. 3. (a) Magnetocapacitive effect in the real part of the dielectric constant ϵ' of $\text{CaMn}_{0.88}\text{Sb}_{0.12}\text{O}_3$ (an ac voltage of 1 V/mm and 100 kHz). (b) Frequency dependence of ϵ' of $\text{CaMn}_{0.9}\text{Sb}_{0.1}\text{O}_3$ (0 T, 1 V/mm).

the peak of $\epsilon'(T)$ is suppressed and shifted to a higher temperature with an increasing frequency.

IV. DISCUSSION

As discussed for $\text{CaMn}_{0.85}\text{Sb}_{0.15}\text{O}_3$ [14], [15], the peak structure of $\epsilon'(T)$ in $\text{CaMn}_{1-x}\text{Sb}_x\text{O}_3$ ($0.1 \leq x \leq 0.2$) suggests that it becomes difficult for the dipole moments to follow the plus-minus switching of an applied ac voltage below T_p . This behavior can be interpreted as the result of a spontaneous dipole ordering. The large value and the broad peak of ϵ' as well as its frequency dependence suggest that $\text{CaMn}_{1-x}\text{Sb}_x\text{O}_3$ is a relaxor in which the polar nanoregions exist in a non-polar matrix [24]. The inevitable disorder induced by substitution is consistent with the relaxor scenario. Since the shoulder structure of $\epsilon''(T)$ is understood as a peak appeared on a quasi-power-law background, the shoulder is expected to indicate a dielectric energy dissipation. These results in $\text{CaMn}_{1-x}\text{Sb}_x\text{O}_3$ ($0.1 \leq x \leq 0.2$) suggest that local dipole-ordering clusters which start to form at T_p expand remarkably around T_s for an energy dissipation to be detectable in ϵ'' . Since some relaxors exhibit ferroelectricity much below the peak temperature of $\epsilon'(T)$, it is expected to be reasonable for dipole-ordering clusters to grow gradually on cooling.

The suppression of the peak height of ϵ' by a magnetic field suggests that the response of dipole moments to an applied

ac voltage is interfered by the magnetic field. In other words, a spontaneous dipole ordering along a certain direction is stabilized by a magnetic field.

In order to discuss the origin of the dielectric anomalies and the magnetocapacitive effect in $\text{CaMn}_{1-x}\text{Sb}_x\text{O}_3$, the $x - T$ phase diagram would be important. Focusing on the dielectric properties, we have newly revealed that T_p and T_s are almost linearly enhanced from $x = 0.1$ to 0.2 . On other properties such as the magnetic phase, we can speculate based on the phase diagram of the similar carrier-doped manganites. Comparing the one-electron-doped system $\text{CaMn}_{1-x}\text{Sb}_x\text{O}_3$ with a two-electron-doped system $\text{AeMn}_{1-z}\text{Mo}_z\text{O}_3$ (Ae : Alkaline earth metal), from the viewpoint of the average valence α of Mn ions, $\text{CaMn}_{0.85}\text{Sb}_{0.15}\text{O}_3$ with $\alpha = +3.82$ and $\text{CaMn}_{0.8}\text{Sb}_{0.2}\text{O}_3$ with $\alpha = +3.75$ correspond to $\text{AeMn}_{0.917}\text{Mo}_{0.083}\text{O}_3$ and $\text{AeMn}_{0.889}\text{Mo}_{0.111}\text{O}_3$, respectively. Considering that the structural phase transition from $Pnma$ to $P2_1/m$ at the room temperature occurs between $\text{CaMn}_{0.85}\text{Sb}_{0.15}\text{O}_3$ and $\text{CaMn}_{0.8}\text{Sb}_{0.2}\text{O}_3$, the phase diagram of $\text{CaMn}_{1-x}\text{Sb}_x\text{O}_3$ is expected to be similar to that of $\text{Ca}_{0.75}\text{Sr}_{0.25}\text{Mn}_{1-z}\text{Mo}_z\text{O}_3$ in which the same structural transition occurs between $z = 0.083$ and 0.111 [2]. In the phase diagram of $\text{Ca}_{0.75}\text{Sr}_{0.25}\text{Mn}_{1-z}\text{Mo}_z\text{O}_3$, the ground state for $0.052 \leq z \leq 0.111$, which corresponds to $0.1 \leq x \leq 0.2$ in $\text{CaMn}_{1-x}\text{Sb}_x\text{O}_3$, is the C-type AFM phase with charge/orbital ordering, whose ordering temperature is linearly enhanced by more than 130 K in this range. In $\text{CaMn}_{0.85}\text{Sb}_{0.15}\text{O}_3$, we really observed a magnetic anomaly that suggests a CO near T_p [14], [15].

Therefore, the dielectric peak in $\text{CaMn}_{1-x}\text{Sb}_x\text{O}_3$, which indicates the formation of a dipole ordering, is expected to have a positive correlation with a charge/orbital ordering. As for the magnetocapacitive effect, since charge/orbital orderings in CaMnO_3 series stabilize a certain magnetic ordering [28], we consider that the dipole ordering related to a charge/orbital ordering is affected by a magnetic field through a magnetic ordering. This magnetic-field-sensitive dielectric peak, which seems to be related to a charge/orbital ordering, is similar to that in the hole-doped system $\text{Pr}_{1-x}\text{Ca}_x\text{MnO}_3$ and

198
199
200
201
202
203
204
205
206
207
208
209
210
211
212
213
214
215
216
217
218
219
220
221
222
223
224
225
226
227
228
229
230
231
232
233
234
235
236

237 $Y_{1-x}Ca_xMnO_3$ [5]–[9], but it is the first example among
238 electron-doped $CaMnO_3$ systems.

239 Concerning the dielectric anomaly in the imaginary
240 part which indicates the active development of electri-
241 cally polarized regions, T_s is notably sensitive to the one-
242 electron-doping Sb substitution in $CaMn_{1-x}Sb_xO_3$, whereas
243 it is not affected by the isovalent Sr substitution in
244 $Ca_{1-y}Sr_yMn_{0.85}Sb_{0.15}O_3$ [15]. From these contrast results,
245 we emphasize that the carrier concentration is a crucial
246 parameter for the expansion of polar nanoregions in the
247 $Ca_{1-y}Sr_yMn_{1-x}Sb_xO_3$ system.

248 As a next issue, it would be important to clarify whether
249 macroscopic electric polarization exists at low temperatures.
250 In order to check our scenario on the mechanism of the
251 dipole anomalies and the magnetocapacitive effect in the
252 $Ca_{1-y}Sr_yMn_{1-x}Sb_xO_3$ system, the magnetic ground state and
253 the possibility of a charge/orbital ordering should be studied.

254 V. CONCLUSION

255 We measured the dielectric constant of the electron-doped
256 manganite $CaMn_{1-x}Sb_xO_3$ ($x = 0.1, 0.12, 0.13, 0.15,$
257 $\text{and } 0.2$). The temperature dependence of the real part exhibits
258 a broad and large peak of which value is suppressed and
259 of which temperature is enhanced by increasing frequency,
260 whereas the imaginary part shows a shoulder anomaly on a
261 quasi-power-law temperature dependence. These results sug-
262 gest that $CaMn_{1-x}Sb_xO_3$ is a relaxor: clusters with a short-
263 range dipole ordering appear at the peak temperature and grow
264 gradually, especially actively at the shoulder temperature.

265 Importantly, we have revealed that the shoulder temperature
266 is remarkably enhanced with the increasing Sb content x .
267 This result indicates that the growth of the clusters is strongly
268 affected by the carrier concentration. Moreover, the dielectric
269 peak is sensitive to a magnetic field in all the samples. By anal-
270 ogy with other $CaMnO_3$ systems, a charge/orbital ordering and
271 an accompanying magnetic ordering might play an important
272 role for the dielectric ordering in $CaMn_{1-x}Sb_xO_3$.

273 ACKNOWLEDGMENT

274 The authors would like to thank Y. Ishii, H. Yamamoto,
275 S. Sekigawa, and H. Kimura for their fruitful discussions. This
276 work was supported in part by Iwate University and in part
277 by JSPS KAKENHI Grant Number JP17K14101.

278 REFERENCES

279 [1] A. Maignan, C. Martin, C. Autret, M. Hervieu, B. Raveau, and
280 J. Hejtmanek, "Structural–magnetic phase diagram of Mo-substituted
281 $CaMnO_3$: Consequences for thermoelectric power properties," *J. Mater.*
282 *Chem.*, vol. 12, no. 6, pp. 1806–1811, 2002.
283 [2] T. Okuda and Y. Fujii, "Cosubstitution effect on the magnetic, transport,
284 and thermoelectric properties of the electron-doped perovskite manganite
285 $CaMnO_3$," *J. Appl. Phys.*, vol. 108, no. 10, p. 103702, 2010.
286 [3] J. L. Cohn, M. Peterca, and J. J. Neumeier, "Low-temperature permittivity
287 of insulating perovskite manganites," *Phys. Rev. B, Condens. Matter*,
288 vol. 70, no. 21, p. 214433, 2004.
289 [4] J. L. Cohn, M. Peterca, and J. J. Neumeier, "Giant dielectric permittivity
290 of electron-doped manganite thin films, $Ca_{1-x}La_xMnO_3$
291 ($0 \leq x \leq 0.03$)," *J. Appl. Phys.*, vol. 97, no. 3, p. 034102, 2005.
292 [5] C. Jardón *et al.*, "Experimental study of charge ordering transi-
293 tion in $Pr_{0.67}Ca_{0.33}MnO_3$," *J. Magn. Magn. Mater.*, vols. 196–197,
294 pp. 475–476, May 1999.

[6] S. Mercene, A. Wahl, A. Pautrat, M. Pollet, and C. Simon, "Anomaly in
295 the dielectric response at the charge-orbital-ordering transition of
296 $Pr_{0.67}Ca_{0.33}MnO_3$," *Phys. Rev. B, Condens. Matter*, vol. 69, p. 174433,
297 May 2004.
298 [7] R. S. Freitas, J. F. Mitchell, and P. Schiffer, "Magnetodielectric conse-
299 quences of phase separation in the colossal magnetoresistance manganite
300 $Pr_{0.7}Ca_{0.3}MnO_3$," *Phys. Rev. B, Condens. Matter*, vol. 72, no. 14,
301 p. 144429, 2005.
302 [8] C. R. Serrao, A. Sundaresan, and C. N. R. Rao, "Multiferroic nature
303 of charge-ordered rare earth manganites," *J. Phys., Condens. Matter*,
304 vol. 19, p. 496217, 2007.
305 [9] J. R. Sahu, C. R. Serrao, A. Ghosh, A. Sundaresan, and C. N. R. Rao,
306 "Charge-order-driven multiferroic properties of $Y_{1-x}Ca_xMnO_3$," *Solid*
307 *State Commun.*, vol. 149, pp. 49–51, Jan. 2009.
308 [10] Y. Murano, M. Matsukawa, S. Kobayashi, S. Nimori, and
309 R. Suryanarayanan, "Transport and magnetic properties of electron-
310 doped manganites $CaMn_{1-x}Sb_xO_3$," *J. Phys., Conf. Ser.*, vol. 200,
311 no. 1, p. 012114, 2010.
312 [11] Y. Murano *et al.*, "Effect of pressure on the magnetic, transport,
313 and thermal-transport properties of the electron-doped manganite
314 $CaMn_{1-x}Sb_xO_3$," *Phys. Rev. B, Condens. Matter*, vol. 83, p. 054437,
315 Feb. 2011.
316 [12] T. Fujiwara, M. Matsukawa, S. Ohuchi, S. Kobayashi, S. Nimori, and
317 R. Suryanarayanan, "Magnetization reversal and chemical pressure effect
318 in the electron-doped manganite $CaMn_{0.95}Sb_{0.05}O_3$," *J. Kor. Phys. Soc.*,
319 vol. 62, p. 1925, 2013.
320 [13] T. Fujiwara *et al.*, "Magnetic and thermodynamic properties of the
321 lightly electron-doped manganite compound $(Ca,Sr)Mn_{0.95}Sb_{0.05}O_3$,"
322 *J. Magn. Magn. Mater.*, vol. 378, pp. 451–456, Mar. 2015.
323 [14] H. Taniguchi, H. Takahashi, A. Terui, S. Kobayashi, M. Matsukawa,
324 and R. Suryanarayanan, "Dielectric anomaly and magnetoelectric effect
325 accompanying a charge ordering in the electron-doped manganite
326 $Ca_{1-x}Sr_xMn_{0.85}Sb_{0.15}O_3$," *J. Phys., Conf. Ser.*, vol. 969, no. 1,
327 p. 012094, 2018.
328 [15] H. Taniguchi, H. Takahashi, A. Terui, S. Kobayashi, M. Matsukawa,
329 and R. Suryanarayanan, "Relaxor-like dielectric anomaly and magneto-
330 capacitive effect in electron-doped $Ca_{1-x}Sr_xMn_{0.85}Sb_{0.15}O_3$," submit-
331 ted for publication.
332 [16] M. Fiebig, T. Lottermoser, D. Fröhlich, A. V. Goltsev, and
333 R. V. Pisarev, "Observation of coupled magnetic and electric domains,"
334 *Nature*, vol. 419, pp. 818–820, Oct. 2002.
335 [17] B. Lorenz, Y.-Q. Wang, and C.-W. Chu, "Ferroelectricity in perovskite
336 $HoMnO_3$ and $YMnO_3$," *Phys. Rev. B, Condens. Matter*, vol. 76, no. 10,
337 p. 104405, 2007.
338 [18] T. Kimura, T. Goto, H. Shintani, K. Ishizaka, T. Arima, and Y. Tokura,
339 "Magnetic control of ferroelectric polarization," *Nature*, vol. 426,
340 pp. 55–58, Nov. 2003.
341 [19] M. Kenzelmann *et al.*, "Magnetic inversion symmetry breaking and
342 ferroelectricity in $TbMnO_3$," *Phys. Rev. Lett.*, vol. 95, no. 8, p. 087206,
343 2005.
344 [20] A. H. Arkenbout, T. T. M. Palstra, T. Siegrist, and T. Kimura, "Ferro-
345 electricity in the cycloidal spiral magnetic phase of $MnWO_4$," *Phys.*
346 *Rev. B, Condens. Matter*, vol. 74, no. 18, p. 184431, 2006.
347 [21] O. Heyer *et al.*, "A new multiferroic material: $MnWO_4$," *J. Phys.,*
348 *Condens. Matter*, vol. 18, no. 39, p. L471, 2006.
349 [22] K. Taniguchi, N. Abe, T. Takenobu, Y. Iwasa, and T. Arima, "Ferro-
350 electric polarization flop in a frustrated magnet $MnWO_4$ induced by a
351 magnetic field," *Phys. Rev. Lett.*, vol. 97, p. 097203, Aug. 2006.
352 [23] W. Kleemann, V. V. Shvartsman, P. Borisov, and A. Kania, "Coexistence
353 of antiferromagnetic and spin cluster glass order in the magnetoelec-
354 tric relaxor multiferroic $PbFe_{0.5}Nb_{0.5}O_3$," *Phys. Rev. Lett.*, vol. 105,
355 p. 257202, Dec. 2010.
356 [24] A. A. Bokov and Z.-G. Ye, "Recent progress in relaxor ferroelectrics
357 with perovskite structure," *J. Mater. Sci.*, vol. 41, no. 1, pp. 31–52, 2006.
358 [25] V. Poltavets, K. Vidyasagar, and M. Jansen, "Crystal structures and
359 magnetic properties of $CaSb_xMn_{1-x}O_3$ perovskites," *Solid State Chem.*,
360 vol. 177, pp. 1285–1291, Apr./May 2004.
361 [26] R. D. Shannon, "Revised effective ionic radii and systematic studies
362 of interatomic distances in halides and chalcogenides," *Acta Cryst.*,
363 vol. 32, pp. 751–767, Sep. 1976.
364 [27] V. K. Shukla, S. Mukhopadhyay, K. Das, A. Sarma, and I. Das, "Direct
365 experimental evidence of multiferroicity in a nanocrystalline Zener
366 polaron ordered manganite," *Phys. Rev. B, Condens. Matter*, vol. 90,
367 no. 24, p. 245126, 2014.
368 [28] E. N. Caspi *et al.*, "Structural and magnetic phase diagram of the
369 two-electron-doped $(Ca_{1-x}Ce_x)MnO_3$ system: Effects of competition
370 among charge, orbital, and spin ordering," *Phys. Rev. B, Condens.*
371 *Matter*, vol. 69, no. 10, p. 104402, 2004.
372